Decision-free radius-directed Kalman filter for universal polarization demultiplexing of square M-QAM and hybrid QAM signals

Yanfu Yang (杨彦甫)[1], Qun Zhang (张 群)[1], Yong Yao (姚 勇)[1,*], Guoliang Cao (曹国亮)[1], Kangping Zhong[2], Xian Zhou[2], Alan Pak Tao Lau[2], and Chao Lu[3]

[1]*Department of Electronic and Information Engineering, Shenzhen Graduate School, Harbin Institute of Technology, Shenzhen 518055, China*

[2]*Photonics Research Center, Department of Electrical Engineering, The Hong Kong Polytechnic University, Hong Kong, China*

[3]*Photonics Research Center, Department of Electronic and Information Engineering, The Hong Kong Polytechnic University, Hong Kong, China*

**Corresponding author: yaoyong@hit.edu.cn*

Received May 18, 2016; accepted September 9, 2016; posted online October 14, 2016

We propose and experimentally demonstrate a universal and blind polarization-state tracking scheme for M-quadrature amplitude modulation (QAM) signals based on a decision-free radius-directed linear Kalman filter (RD-LKF). The polarization tracking performance is investigated through simulation and experiments for both quadrature phase-shift keying (QPSK) and 16-QAM signals. The influence of the filter parameters on the static polarization demultiplexing performance and dynamic tracking capability are discussed via simulation. The optimization strategy of the filter parameters in modulation-format-independent scenarios is proposed and simulations are carried out to evaluate the polarization demultiplexing penalty for QPSK, 16QAM, and hybrid QPSK/16QAM signals. Finally, the proposed decision-free RD-LKF is experimentally compared to the respective algorithms of constant modulus algorithm and multimodulus algorithm for QPSK and 16-QAM and the advantage of ultrafast polarization tracking ability is confirmed.

OCIS codes: 060.1660, 120.3930.
doi: 10.3788/COL201614.110601.

Rate adaptive transceivers have recently attracted much attention due to their potential for improving overall optical network efficiency under dynamic internet traffic patterns in emerging data center or various cloud applications. The spectral efficiency of the transmitter may be adjusted discretely by configuring quadrature amplitude modulation (QAM) formats or may be tuned continuously with time domain hybrid QAM (TDHQ) schemes[1–3]. Therefore, universal digital signal processing (DSP) schemes supporting dynamic modulation formats is gaining more and more attention[4,5]. In a polarization-division-multiplexing (PDM) coherent receiver, fast polarization tracking and demultiplexing is an indispensable DSP module to deal with rapid stokes vector movements caused by external vibrations[6]. Compared with training sequence (TS) methods, blind polarization demultiplexing may be desired due to a high spectral efficiency and no frame synchronization. Conventional blind polarization demultiplexing algorithms, including the constant modulus algorithm (CMA)[7], the multimodulus algorithm (MMA), and their variants[8], have been applied to PDM-quadrature phase-shift keying (QPSK) and PDM-16QAM, respectively. However, these schemes are modulation format dependent and a universal scheme applicable for dynamic optical signals is highly desired. Gao *et al.* proposed a two-stage universal demultiplexing scheme employing CMA-based preconvergence and decision-directed least mean square (DD-LMS) together[5]. Recently, due to its excellent estimation accuracy and tracking ability, the Kalman filter has attracted much attention for coherent optical systems. The reported application examples include clock tone enhancement[9], carrier recovery[10–12], and polarization tracking[13–15]. We proposed a novel radius-directed linear Kalman filter (RD-LKF) scheme for fast polarization tracking that is immune to frequency offset compared to the previous extended Kalman filter (EKF) scheme[13]. Here, we further modify our proposed RD-LKF scheme into a universal polarization-state tracking framework for dynamic modulation formats.

In this Letter, a universal polarization-state tracking based on a decision-free RD-LKF filter is proposed and experimentally investigated for M-QAM formats. The universal RD-LKF-based scheme has the constant radius as a reference for the residual estimation regardless of the modulation order of M-QAM signals. Consequently, the scheme involves no radius decision operation and can work in a universal manner. As an application extension of RD-LKF, this universal scheme has inherently the advantages of immunity to the carrier phase, frequency offset, and singularity problem. The rest of the Letter is organized as follows. First, the principle of the decision-free RD-LKF scheme is introduced. The polarization demultiplexing

performance of the proposed universal scheme is then investigated via numerical simulations for PDM-QPSK, PDM-16QAM signals, and TDHQ signals. The influences of the filter tuning parameters on tracking performance are discussed in detail and the strategy of choosing a unified parameter for dynamic scenarios is proposed. Finally, the decision-free RD-LKF scheme is experimentally studied and the tracking performance of the proposed scheme and the CMA/MMA algorithms are compared for PDM QPSK/16-QAM signals, respectively.

We consider typical polarization-multiplexed transmissions[13] and the received signals $\boldsymbol{Z}(t)$ have the expression

$$\boldsymbol{Z}(t) = \alpha \boldsymbol{J}(t)[\boldsymbol{X}(t) \cdot e^{j(\Delta\omega t)} \cdot e^{j\theta(t)} + \xi(t)], \tag{1}$$

where $X(t), \boldsymbol{Z}(t), \Delta\omega, J(t), \theta(t), \alpha, \xi(t)$ describe the transmitted signal, the received signal, frequency offset, time-varying Jones matrix, carrier phase noise, fiber loss factor, and additive white Gaussian noise in dual polarization. The polarization demultiplexed signal $\boldsymbol{U}(t)$ can be expressed as follows:

$$\begin{aligned}\boldsymbol{U}(t) &= \boldsymbol{X}(t) \cdot e^{j(\Delta\omega t)} \cdot e^{j\theta(t)} + \xi(t) = [\alpha \boldsymbol{J}(t)^{-1}]\boldsymbol{Z}(t) \\ &= \begin{bmatrix} a(t)+jb(t) & c(t)+jd(t) \\ -c(t)+jd(t) & a(t)-jb(t) \end{bmatrix} \begin{bmatrix} Z_x(t) \\ Z_y(t) \end{bmatrix}. \end{aligned} \tag{2}$$

Four real variables $\{a \quad b \quad c \quad d\}$ are related to the polarization inversion matrix estimated by the Kalman filter. After time discretization with $t = kTs$ (Ts is the symbol period), the polarization demultiplexed signal $\boldsymbol{U}(k)$ can be rewritten as the product of $\boldsymbol{H}(k)$ and $\boldsymbol{S}(k)$, which has the expressions shown in Eqs. (3) and (4). In Eq. (5) the measurement prediction $\boldsymbol{U}(k)$ is expressed by the product of $\boldsymbol{H}(k)$ and $\boldsymbol{S}(k)$ and $\boldsymbol{v}(k)$ represents the measurement noise. The process equation in Eq. (6) describes the state vector $\boldsymbol{S}(k)$ and $\boldsymbol{w}(k)$ represents the process noise. The state vector $\boldsymbol{S}(k)$ will be estimated in an iterative manner under the Kalman filter framework based on the Kalman prediction in Eqs. (7) and (8) and the Kalman update in Eqs. (9)–(12)[16]. $\boldsymbol{P}^{-}(k)$, $\boldsymbol{P}(k)$, $\Delta\boldsymbol{U}(k)$, and $\boldsymbol{K}(k)$ are called priori estimate error covariance, posteriori estimate error covariance, residual, and Kalman gain, respectively. The tuning parameters of $\boldsymbol{Q}$ and $\boldsymbol{R}$ describe the process noise covariance and measurement noise covariance and can be considered as scaled identities. They should be set at proper values for optimal estimation performance in practice.

$$\boldsymbol{H}(k) = \begin{bmatrix} Z_x(k) & jZ_x(k) & Z_y(k) & jZ_y(k) \\ Z_y(k) & -jZ_y(k) & -Z_x(k) & Z_x(k) \end{bmatrix}, \tag{3}$$

$$\boldsymbol{S}(k) = [\, a(k) \quad b(k) \quad c(k) \quad d(k) \,]^T, \tag{4}$$

$$\boldsymbol{U}(k) = \boldsymbol{H}(k)\boldsymbol{S}(k) + \boldsymbol{v}(k), \tag{5}$$

$$\boldsymbol{S}(k) = \boldsymbol{S}(k-1) + \boldsymbol{w}(k), \tag{6}$$

$$\boldsymbol{S}^{-}(k) = \boldsymbol{S}(k-1), \tag{7}$$

$$\boldsymbol{P}^{-}(k) = \boldsymbol{P}(k-1) + \boldsymbol{Q}, \tag{8}$$

$$\boldsymbol{K}(k) = \boldsymbol{P}^{-}(k)\boldsymbol{H}^{T}(k)[\boldsymbol{H}(k)\boldsymbol{P}^{-}(k)\boldsymbol{H}^{T}(k) + \boldsymbol{R}]^{-1}, \tag{9}$$

$$\Delta\boldsymbol{U}(k) = \boldsymbol{U}_{\boldsymbol{c}}(k) - \boldsymbol{U}(k) = \boldsymbol{U}_{\boldsymbol{c}}(k) - \boldsymbol{H}(k)\boldsymbol{S}^{-}(k), \tag{10}$$

$$\boldsymbol{S}(k) = \boldsymbol{S}^{-}(k) + \boldsymbol{K}(k)\Delta\boldsymbol{U}(k), \tag{11}$$

$$\boldsymbol{P}(k) = \boldsymbol{P}^{-}(k) - \boldsymbol{K}(k)\boldsymbol{H}(k)\boldsymbol{P}^{-}(k). \tag{12}$$

The schematic diagram of the filtering process is plotted in Fig. 1. In each iteration, the measurement prediction $\boldsymbol{U}(k)$ is first computed with the state prediction $\boldsymbol{S}^{-}(k)$ and the input signal $\boldsymbol{Z}(k)$. In the proposed decision-free RD-LKF implementation, the circle with a constant radius is employed as the tracking target of the measurement prediction during the update of the state vector. As shown in the inset of Fig. 1, the reference vector $U(k)$ on the target circle has the same phase angle as $\boldsymbol{U}_{\boldsymbol{c}}(k)$. The resultant residual of $\Delta\boldsymbol{U}(k) = \boldsymbol{U}_{\boldsymbol{c}}(k) - \boldsymbol{U}(k)$ represents the radial displacement between the measurement prediction and the reference. It is worth noting that in our previous work[15] different Kalman filter implementations were employed for the following modulation formats: single measurement equation with a fixed target circle is used for QPSK signals; double measurement methods are employed for 16QAM signals and the second measurement involves three radii values for decision usage. In this Letter, single measurement with the same target circle is applied for different formats. Therefore, the scheme is inherently free of decision operation during the state update and can be implemented in a universal architecture. In the following, the universal RD-LKF will be investigated in detail through both simulation and experimental verifications to prove its feasibility for QPSK, 16QAM, and even time domain QPSK/16QAM hybrid signals. It is worth noting that the same target radius, the same tuning parameters, and the same signal normalization will be employed to achieve universal polarization tracking regardless of modulation format.

First, the preliminary simulation results of polarization demultiplexing of PDM-QPSK, 16QAM, 64QAM, and

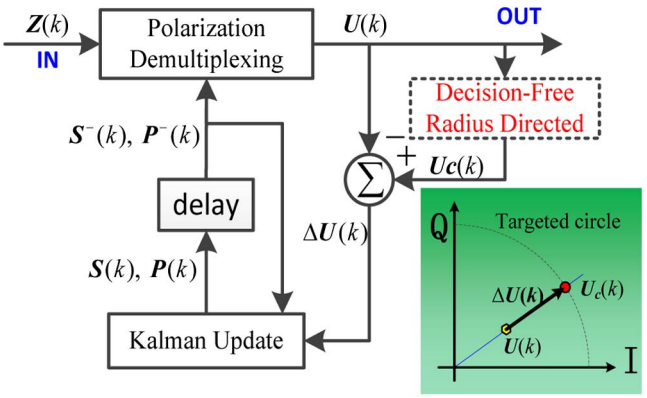

Fig. 1. Block diagram for the proposed polarization demultiplexing and tracking algorithm.

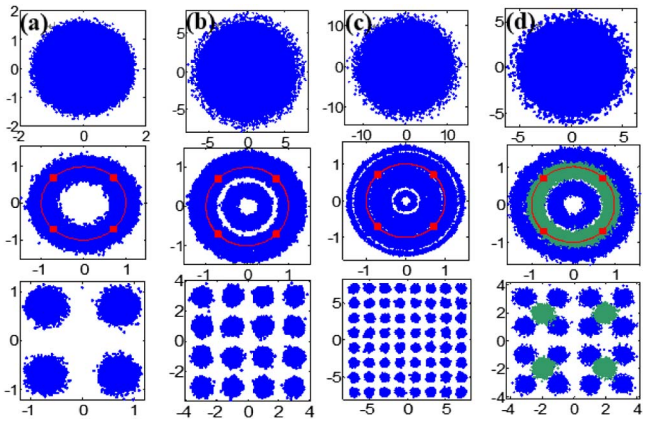

Fig. 2. Constellation diagrams of before demultiplexing, after demultiplexing, and carrier phase recovery for (a) PDM-QPSK, (b) PDM-16QAM, (c) PDM-64QAM, and (d) PDM-hybrid-QPSK/16QAM (red line is the targeted circle).

QPSK/16QAM hybrid signals are presented in Fig. 2. The normalized power of 1.0 and the target radius of 1.0 are used for all formats in a universal manner. It can be seen from the constellation diagrams that successful polarization demultiplexing is achieved for all formats including QPSK/16QAM hybrid signals.

In the following, the influence of the tuning parameters on performance is discussed through simulation with example formats of QPSK and 16-QAM. $\boldsymbol{Q}$ and $\boldsymbol{R}$ can directly or indirectly adjust the Kalman gain K and consequently the ratio between the prediction and the residual during the Kalman update. $\boldsymbol{Q}$ and $\boldsymbol{R}$ are simplified to be a diagonal matrix and the diagonal values (represented by Q and R) are only analyzed in the following. For simplicity, R is set to the fixed value of 0.1 and only Q is used to optimize the filter performance. Figure 3 presents the bit error ratio (BER) as a function of polarization rotation angular frequency under different Q parameters in 112 Gb/s PDM-QPSK and PDM-16QAM systems. In the simulation, the Jones matrix of polarization rotation is used[17]. The optical signal-to-noise ratio (OSNR) is set at 14 and 17.5 dB for QPSK and 16QAM, respectively. The proposed Kalman filter is used for polarization tracking and demultiplexing and the ideal carrier recovery compensation is assumed. The influence of Q on the polarization tracking performance is similar for QPSK and 16QAM signals. In the quasi-static polarization state or slow rotation regime, a smaller Q is preferred for better estimation accuracy performance. However, in the high-speed rotation regime, a larger Q is desired for better tracking ability. The dependence of polarization tracking on the tuning parameter is very similar to that of CMA-based demultiplexing on the step size[17]. Therefore, the tuning parameter should be chosen around a moderate value for each format to obtain the performance balance in two aspects: (a) the small acceptable penalty at the slow rotation regime and (b) the tracking capability as fast as possible.

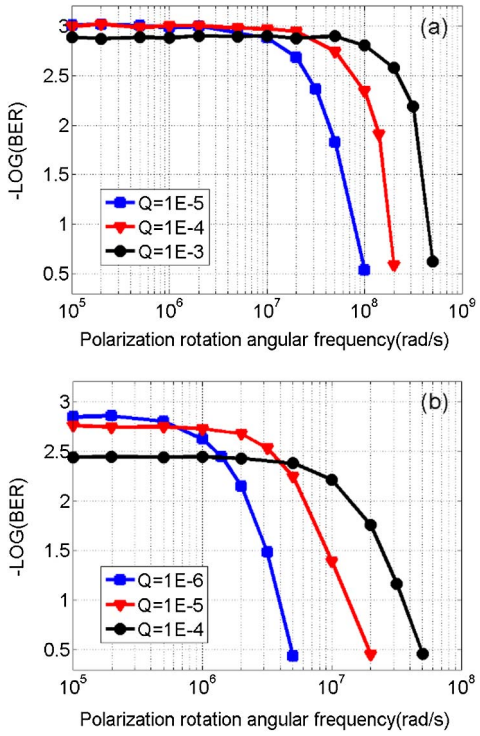

Fig. 3. BER vs. polarization rotation angular frequency with different Q parameters for (a) PDM-QPSK and (b) PDM-16QAM.

In the following, we will discuss how to choose a unified parameter for universal tracking of QPSK and 16QAM signals. This issue has to be dealt with because the receiver has no prior information on the modulation format in a dynamic optical network. By a comparison between Figs. 3(a) and 3(b), it is found that the optimized parameter is slightly different for two formats. Considering the inherent better tracking performance in the lower-order format and the high tolerance against the filter parameter, the unified parameter should be configured with the priority to the higher-order format. As an example of this strategy, the Q of 1×10^{-5} is chosen for the following simulation and experiments based on the resultant trade-off: (a) in the 16-QAM case, the performance balance between the estimation accuracy and the tracking ability is well achieved; (b) in the QPSK case, the slightly degraded tracking performance is acceptable because it is still far beyond the tracking speed in 16QAM.

Next, the static polarization demultiplexing performance of the proposed decision-free RD-LKF is presented in Fig. 4 for 28 GS/s QPSK, 14 GS/s 16QAM, and TDHQ (18.7 GS/s, QPSK/16QAM format ratio [1:1], power ratio [1:5]) signals, respectively. In the simulation, the polarization-related Jones matrix is static and the unified parameter of $Q = 1 \times 10^{-5}$ and $R = 0.1$ are used for all signals. In the QPSK case, a perfect polarization demultiplexing is achieved and the OSNR penalty can be ignored. In the 16QAM and hybrid signal cases there exists a small polarization demultiplexing (PolDemux) induced penalty of less than 0.3 dB with the BER of 1×10^{-3}. In addition, the 16QAM demultiplexing performance with a double

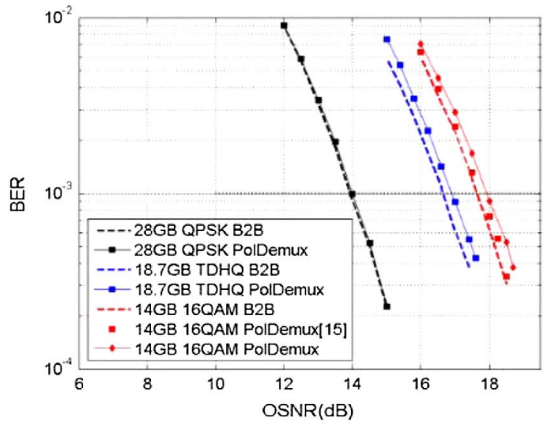

Fig. 4. Simulated BER versus OSNR for the 112 Gb/s PDM-QPSK (28 GB), PDM-16QAM (14 GB), and THDQ signals (QPSK/16QAM) with the proposed universal polarization methods. The 16QAM results with the methods proposed in Ref. [15] are also presented for comparison.

measurement RD-LKF[15] is also provided. As a comparison, the universal decision-free RD-LKF has an extra penalty of around 0.25 dB due to the simplified target circle of one constant radius.

The OSNR penalty as a function of the polarization rotation angular frequency is simulated with the proposed universal RD-LKF scheme applied in the 112 Gb/s PDM-QPSK and PDM-16QAM signals. As shown in Fig. 5, with the 1 dB OSNR penalty, the universal RD-LKF can track the maximum polarization rotation of around 40 Mrad/s for QPSK and around 3.5 Mrad/s for 16QAM.

The proposed decision-free RD-LKF scheme is also experimentally studied in a 112 Gb/s coherent optical communication system with a flexible PDM-QPSK or PDM-16QAM signal transmitter, as shown in Fig. 6. An the optical I/Q modulator is driven by a 28 GS/s 2-level signal for QPSK generation or a 14 GS/s 4-level signal for 16QAM generation with an electrical arbitrary waveform generator. The coherent detected signals are sampled by a real-time oscilloscope at 50 GS/s in QPSK and 80 GS/s in

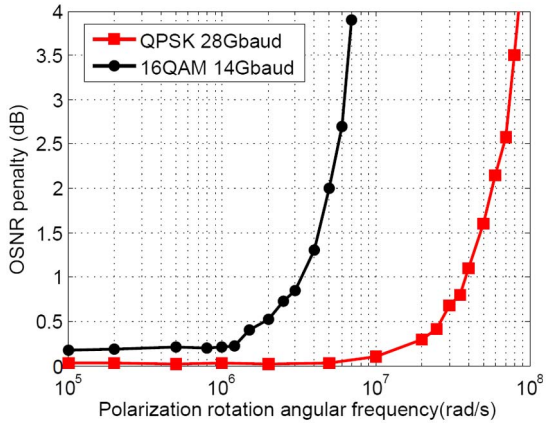

Fig. 5. Simulated OSNR penalty vs. polarization rotation angular frequency for 112 Gb/s PDM-QPSK and PDM-16QAM.

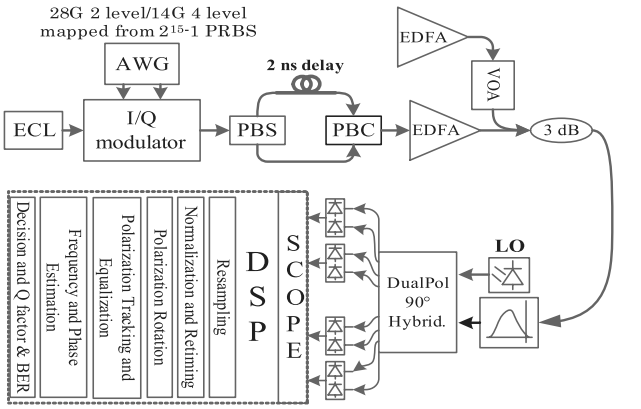

Fig. 6. Experimental scheme and digital processing of the 112 Gb/s PDM-QPSK/PDM-16QAM coherent optical communication system.

16QAM. The endless polarization rotation was digitally achieved by a polarization rotation matrix in the DSP section before polarization demultiplexing[17]. The sampled data was processed offline and the polarization tracking algorithms may be one of the decision-free RD-LKF, CMA, and MMA for comparison. The Q-factor is calculated from 5 independently acquired 56000 symbols.

The tracking performance of the universal decision-free RD-LKF is investigated experimentally. The unified parameter of Q is fixed at 1×10^{-5} for both QPSK and 16QAM signals. Figure 7(a) represents the comparison between the decision-free RD-LKF and CMA for PDM-QPSK. The taps and step size u of CMA are set to 3

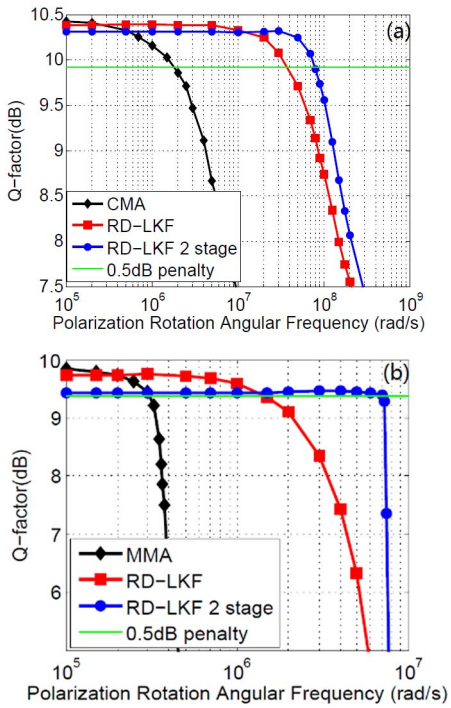

Fig. 7. Q-factor performance versus polarization rotation angular frequency for (a) QPSK and (b) 16QAM.

and 10^{-4}, respectively. With the 0.5 dB Q-factor penalty, the decision-free RD-LKF can track the polarization rotation angular frequency at 38 Mrad/s. Figure 7(b) represents the comparison between the decision-free RD-LKF and MMA for PDM-16QAM. The taps, step size u of MMA is set to 3 and 10^{-4}, respectively. With the 0.5 dB Q-factor penalty, the decision-free RD-LKF can track the polarization rotation up to 1.6 Mrad/s. Different from the double measure method employed in 16QAM[15], the single measurement equation with one constant target radius is used. Compared to the result in Ref. [15], this decision-free RD-LKF has a 0.3 dB Q-factor degradation in the slow polarization rotation regime and also has a slight degradation on tracking capability. In addition, the tracking performance improvement by cascading two decision-free RD-LKF is achieved.

In conclusion, a universal decision-free RD-LKF scheme is proposed and demonstrated experimentally for tracking the polarization state of square multilevel QAM and TDHQ signals. As an illustration example, the scheme is applied in a universal manner for QPSK, 16QAM, and QPSK/16QAM hybrid signals. The simulation results show that in either the QPSK or 16QAM system, the filter tuning parameter should be moderate to obtain the balance between the demultiplexing penalty under the slow-varying polarization state and high-speed tracking capability. Considering a universal application, the unified filter parameters should be chosen with the priority to a higher-order QAM, which has a relatively worse tracking ability and is more sensitive to the filter parameter compared to the lower-order format. With the chosen parameters, the simulation results show that the decision-free RD-LKF can achieve successful demultiplexing of three kinds of signals in a universal manner with less than a 0.3 dB penalty. Meanwhile, the polarization tracking speeds of 40 and 3.5 Mrad/s are obtained for QPSK and 16QAM signals, respectively. Finally, the universal RD-LKF scheme is experimentally compared to the conventional algorithms and the fast tracking capability is confirmed.

This work was supported by the National Natural Science Foundation of China (Nos. 61205046, 61401020, and 61575051), the Shenzhen Municipal Science and Technology Plan Project (Nos. JCYJ20150327155705357, KQCX2015032409501296, and JSGG20150529153336124, and JCYJ20150529114045265), and the Hong Kong Government General Research Fund (GRF) (No. PolyU 152079/14E).

References

1. Q. Zhuge, M. Morsy-Osman, X. Xu, M. Chagnon, M. Qiu, and D. V. Plant, J. Lightwave Technol. **31**, 2621 (2013).
2. A. P. T. Lau, Y. Gao, Q. Sui, D. Wang, Q. Zhuge, M. Morsy-Osman, M. Chagnon, X. Xu, C. Lu, and D. V. Plant, IEEE Signal Process. Mag. **31**, 82 (2014).
3. Z. He, W. Liu, B. Shen, X. Chen, X. Gao, S. Shi, Q. Zhang, D. Shang, Y. Ji, and Y. Liu, Chin. Opt. Lett. **14**, 0406024 (2016).
4. Y. Sun, L. Xi, X. Tang, D. Zhao, Y. Qiao, X. Zhang, and X. Zhang, Chin. Opt. Lett. **12**, 100606 (2014).
5. Y. Gao, Q. Zhuge, D. V. Plant, C. Lu, and A. P. T. Lau, in *Proceedings of the Optical Fiber Communication Conference (OFC-2014)* (2014), paper Th3E.5.
6. P. M. Krummrich and K. Kotten, in *Proceedings of the Optical Fiber Communication Conference (OFC-2004)* (2004), paper FI3.
7. J. Xiao, C. Tang, X. Li, J. Yu, X. Huang, C. Yang, and N. Chi, Chin. Opt. Lett. **12**, 050603 (2014).
8. I. Fatadin, D. Ives, and S. J. Savory, J. Lightwave Technol. **27**, 3042 (2009).
9. W. Ng, A. T. Nguyen, C. S. Park, and L. A. Rusch, in *Proceedings of the Optical Fiber Communication Conference (OFC-2015)* (2015), paper Th2A.19.
10. M. I. Olmedo, X. Pang, M. Piels, R. Schatz, G. Jacobsen, S. Popov, I. Tafur Monroy, and D. Zibar, in *Proceedings of the Optical Fiber Communication Conference (OFC-2015)* (2015), paper Th2A.10.
11. L. Pakala and B. Schmauss, in *Proceedings of the European Conference on Optical Communication (ECOC-2014)* (2014).
12. T. Inoue and S. Namiki, Opt. Exp. **22**, 15376 (2014).
13. T. Marshall, B. Szafraniec, and B. Nebendahl, Opt. Lett. **35**, 2203 (2010).
14. B. Szafraniec, T. S. Marshall, and B. Nebendahl, J. Lightwave Technol. **31**, 648 (2013).
15. Y. Yang, G. Cao, K. Zhong, X. Zhou, Y. Yao, A. P. T. Lau, and C. Lu, Opt. Express **23**, 19673 (2015).
16. G. Welch and G. Bishop, in *Proceedings of the SIGGRAPH Course* (2001).
17. S. J. Savory, Opt. Express **16**, 804 (2008).